https://doi.org/10.5194/bg-2020-223
Preprint. Discussion started: 3 July 2020

Biogeosciences Discussions

New Insight to Niche Partitioning and Ecological Function of Ammonia Oxidizing Archaea in Subtropical Estuarine Ecosystem

Yanhong Lu[1,2,†], Shunyan Cheung[2,†], Ling Chen[3], Shuh-Ji Kao[3], Xiaomin Xia[4], Jianping Gan[1], Minhan Dai[3], Hongbin Liu[2,5]

[1]SZU-HKUST Joint PhD Program in Marine Environmental Science, Shenzhen University, Shenzhen, China
[2]Department of Ocean Science, The Hong Kong University of Science and Technology, Hong Kong, China
[3]State Key Laboratory of Marine Environmental Science, Xiamen University, China
[4]Key Laboratory of Tropical Marine Bio-resources and Ecology, South China Sea Institute of Oceanology, Chinese Academy of Sciences, Guangzhou, China
[5]Hong Kong Branch of Southern Marine Science & Engineering Guangdong Laboratory, The Hong Kong University of Science and Technology, Hong Kong, China
†These authors shared equal contributions

Correspondence to: Hongbin Liu (liuhb@ust.hk)

https://doi.org/10.5194/bg-2020-223
Preprint. Discussion started: 3 July 2020

Biogeosciences Discussions

Abstract. Nitrification plays a central role in estuarine nitrogen cycle. Previous studies in estuary mainly focused on the niche-partition between ammonia-oxidizing archaea (AOA) and bacteria (AOB), while the diversity, activity, biogeography and ecophysiology of different AOA groups remained unclear. Here, we first time reported niche partitioning as well as differentially distributed active populations among diverse AOA (inferred from *amoA* gene) in a typical subtropical estuary–Pearl River estuary (PRE). In the water column of PRE, the AOA communities mainly consisted of WCA and SCM1-like sublineages. Surprisingly, we observed a strong disagreement of AOA communities at DNA and RNA levels. In DNA samples, WCA generally dominated the AOA community, and the distributional pattern indicated that WCA I and WCA II sublineages preferred oceanic and coastal conditions, respectively. In contrast, diverse SCM1-like sublineages were identified and outnumbering WCA at RNA level, in which SCM1-like-III was limited to freshwater while the rest sublineages were widely distributed in the estuary. The SCM1-like sublineages strongly correlated with nitrification rate indicated their important contribution to ammonia oxidation. Furthermore, intense nitrification contributed significantly to hypoxia conditions (nitrification contributed averaged 15.30 % of oxygen consumption) in the estuary. These results unraveled different ammonia-oxidizing activities and niche partitioning among different AOA sublineages in estuarine water, which was unexplored in previous DNA and clone library-based studies. The ecological significance and functioning of the diverse AOA should be further explored in the marine ecosystem.

https://doi.org/10.5194/bg-2020-223
Preprint. Discussion started: 3 July 2020


Biogeosciences Discussions

1 Introduction

Nitrification, is a microbial mediated oxidation process of ammonia to nitrate, interconnects the source (N-fixation), and sink (N-loss) and plays a central role in the marine nitrogen cycling (Ward 1996). Particularly in the estuarine ecosystem, nitrification significantly impacts the N source for primary production and oxygen level in the water column (Yool et al. 2007; Erguder et al. 2009; Campbell et al. 2019). Regarding the biogeochemical significance of ammonia oxidation (i.e. first and rate-determining step of nitrification) in the estuarine ecosystem, the physiology and ecological function of ammonia oxidizers (i.e. ammonia-oxidizing archaea (AOA) and bacteria (AOB)) have been the major interest to understand the estuarine N transformation (Bernhard and Bollmann 2010). The previous studies were mostly conducted in sediment compared to water columns in estuarine ecosystems (summarized in Table S1) (Damashek et al. 2016). Besides, those studies were mainly focusing on the niche partition between AOA and AOB inferred from *amoA* genes abundance and collectively showed the AOA outnumbered AOB in the estuarine ecosystem (Caffrey et al. 2007; Abell et al. 2010; Bernhard et al. 2010). However, the biogeography, niche partition, and ecological function of different AOA groups were little analyzed (Table S1).

As revealed by *amoA* gene (ammonia monooxygenase subunit A), the marine AOA was early recognized as three major groups, including water column A (WCA; shallow ecotype dominant in epipelagic and upper mesopelagic water) and water column B (WCB; deep ecotype dominant in the mesopelagic and bathypelagic water) and SCM1-like (affiliated to the first isolated AOA–*Nitrosopumilus maritimus* SCM1), in which the distribution and abundance of WCA and WCB were much more studied than SCM1-like ecotype in the field observations (Francis et al. 2005; Hallam et al. 2006; Beman et al. 2008; Beman et al. 2012). The WCA, WCB, and SCM1-like were corresponding to the group NP-Epsilon, NP-Alpha, and NP-Gamma respectively, in the global synthesis of Alves et al. 2018 (Alves 2018; Cheung et al. 2019). More recently, highly diverse sublineages of WCA and WCB were revealed in the global ocean, in which the sublineage within the same ecotype displayed varied distributional patterns and environmental determinants (Cheung et al. 2019). On the other hand, most of the marine AOA remained uncultivated which hinder our understanding of the ecophysiology of most of AOA in marine ecosystems (Alves et al. 2018). Therefore, the physiological understanding of marine AOA (especially WCA and WCB) heavily relied on field observations. Given that highly diverse uncultivated AOA sublineages have been recently defined, their ecophysiology and environmental determinants required further exploration in the environment. For example, niche partitioning between WCB sublineages has been recently observed in the oxygen minimum zone off the Costa Rica Dome and potential anoxic adapted phylotypes were widely detected between the geographically distant OMZs (Lu et al. 2019).

As mentioned, dynamics and ecological function of different AOA were rarely studied in the estuarine water comparing to the relatively well-characterized population in the ocean, sediment, and soil environment (Bernhard and Bollmann 2010; Damashek et al. 2016). Besides, the previous studies of marine AOA mostly relied on clone library analysis (summarized in Table S1), which were insufficient to recover the diversity and biogeography of AOA. Moreover, previous studies largely relied on DNA surveys leaving the relatively active communities in the RNA unexplored. Recently, Wu et al. reported the

https://doi.org/10.5194/bg-2020-223
Preprint. Discussion started: 3 July 2020

differentially transcriptional activities of AOA communities referred from DNA and RNA extracts suggesting the overwhelming studies depended on DNA may have overlooked active groups in the natural environment (Wu et al. 2017). In this study, we have conducted a comprehensive study about ammonia oxidizers in a typical subtropical estuary-Pearl River estuary (PRE) which is the second largest river in China in terms of freshwater discharge (Zhao 1990). During the wet season, Pearl River estuary is characterized by receiving 80 % of annual freshwater discharge forming a typical salt-wedge estuary (Harrison et al. 2008). Recently, reoccurring bottom hypoxia formation at the lower estuary of PRE has received increasing concerns about its ecological impact on the estuarine ecosystem (Qian et al. 2018). The steep natural gradient of salinity, nutrient, oxygen concentration, turbidity makes Pearl River estuary to be an ideal environment to study the diversity and ecological function of ammonia oxidizers. Together, by revealing AOA community structure (dominant ammonia oxidizer) at DNA and RNA level by Ion torrent sequencing and fine-scale phylogenetic classification along with quantification of AOA and AOB and nitrification rate measurement, we aim to 1) identify the major and active AOA in the estuarine ecosystem; 2) identify niche partitioning between different AOA sublineages based on ecophysiology and environmental determinants; 3) determine the potential contribution of nitrification to hypoxia formation in PRE.

2 Materials and methods

2.1 Sample collection

The cruise was conducted from July 11-August 1 in 2017 on the R/V Hai Ke 68. In the first leg, 83 stations designed along the isobath of the 10-50m by 10m interval covered from the upper estuary to the continental shelf (Fig. S1). Water samples were collected using a Niskin bottle equipped with CTD sensor (Sea-Bird SBE 917plus). Temperature, salinity, and depth data were acquired through the CTD sensor. The dissolved oxygen concentrations were measured on board using Winkler Spectrophotometric and titration method, as described in (Pai et al. 2001; Dai et al. 2006). Dissolved inorganic nutrient samples were filtered through the pre-acid washed cellulose acetate fiber membranes and stored in -20 ℃ until analysis in a land-based laboratory in Xiamen University (Qian et al. 2018). Ammonia concentration was determined on board using the indophenol blue spectrophotometric method (Pai et al. 2001). Chlorophyll samples (250 to 500ml) were filter onto GF/F (Whatman, USA) and soon stored in foil bags in liquid nitrogen. Chlorophyll-*a* concentration was measured on Turner Fluorometer (Welschmeyer 1994) after extracted with 90 % acetone for 14 h at -20 ℃. The bacterial abundances were quantified by the Becton-Dickson FACSCalibur flow cytometer (Vaulot et al. 1989). Sea water was prefilter by 20 μm mesh and fixed by final concentration of 0.5 % seawater buffed paraformaldehyde in cryotubes and stored in liquid nitrogen until analysis (Liu et al. 2014). At each sampling depth, 0.5-2 L of sea water were sequentially filtrated onto 3 μm polycarbonate membranes (GVS, USA) for particle-attached community and 0.2 μm polycarbonate membranes for the free-living community. DNA/RNA samples immersed in 500 μl RNAlater (Ambion, Austin, TX, USA) before stored in liquid nitrogen.

https://doi.org/10.5194/bg-2020-223
Preprint. Discussion started: 3 July 2020


Biogeosciences Discussions

92 **2.2 Rates measurement**

93 Community respiration rates were measured through the dissolved oxygen variance before and after 24 h dark incubation in
94 running seawater. The dissolved oxygen concentration was determined by the Winkler titration method (Oudot et al. 1988).
95 Nitrification was measured through 6-12 h dark incubations conducted in a 200ml HDPE bottle added with $^{15}NH+4$ (less 10 %
96 of ambient concentration) in running seawater. The $\delta^{15}N$ in NO- x the product of nitrification, was determined using the
97 denitrifier method (Sigman et al. 2001; Casciotti et al. 2002; Knapp et al. 2005). Nitrification rate is adopted from another
98 study conducted during the same cruise (L. Chen et al. in review). We analyzed the correlation between nitrification rates
99 and AOA sublineages. Equation 1 and 2 were generally considered as the sequential oxidation of ammonia to nitrate.
100 Inferred from the nitrification rates, we estimated the nitrification oxygen demand (NOD) based on equations 1 and 2.
101 Inferred from the nitrification rates, we estimated the nitrification oxygen demand (NOD) based on equation 3 coupling with
102 carbon assimilation (Dai et al. 2006; Dai et al. 2008). We used NOD/CR ratio (percentage) to evaluate potential the
103 contribution of nitrification to total oxygen consumption in the field.

104 $$NH_3 + O_2 \rightarrow NO_2^- + 3H^+ + 2e^- \quad (1)$$

105 $$NO_2^- + H_2O \rightarrow NO_3^- + 2H^+ + 2e^- \quad (2)$$

106 $$NH_4^+ + 1.89O_2 + 1.98HCO_3^- \rightarrow 0.984NO_3^- + 0.016C_5H_7O_2N + 1.90CO_2 + 2.93H_2O \quad (3)$$

107 **2.3 DNA and RNA extraction and cDNA synthesis**

108 The sample filters immersed in RNAlater were thawed on ice. RNAlater was removed following the procedure described in
109 Xu et al. 2013 (Xu et al. 2013). For DNA extraction, filters were cut into pieces and carefully collected into the 2ml Lysing
110 Matrix E tubes with the addition of 978 µl sodium phosphate buffer and 122 µl MT buffer provided in FastDNA™ SPIN Kit
111 for Soil (MP Biomedical, Solon, OH, USA). The lysing matrix was homogenized by Mini-Beadbeater-24 (Biospec Product,
112 Bartlesville, OK, USA), at 3500 oscl/min for 60 seconds. The subsequent procedures of DNA extraction were performed
113 according to FastDNA Spin kit for soil manufacture's instruction and preserved at -80 ℃. For RNA extraction, sample filters
114 were incubated in 1 ml TRIzol for 5 min at room temperature in 2ml sterile microcentrifuge tubes. After the incubation, 200
115 µl chloroform was added into tubes and mixed vigorously by hand until the membrane fully dissolved. After 3 min room
116 temperature incubation, the samples were centrifuged at 12000 × g at 4 ℃ for 15 min. The supernatant was carefully
117 transpired into a new 2ml microcentrifuge and mixed with an equal volume of 70 % ethanol. The purification and elution
118 procedures were performed according to the manufacture's instruction of the PureLink RNA Mini Kit (Life Technologies,
119 Carlsbad, CA, USA). RNA samples were immediately treated with DNase at 37 ℃ for 30 min using the TURBO DNA-free
120 Kit to eliminate DNA contamination. After incubation, the DNase was inactivated following the manufacturer's instruction.
121 The DNA-free RNA samples were reversely transcribed into cDNA with random primers using the SuperScript III First-
122 Strand Synthesis System (Life Technologies, Carlsbad, CA, USA). The synthesized cDNA was further treated with RNase H
123 at 37 ℃ for 20 min to remove the residual RNA.

https://doi.org/10.5194/bg-2020-223
Preprint. Discussion started: 3 July 2020

2.4 PCR amplification and high throughput sequencing

The DNA and cDNA were used as templates in PCR amplification. The archaeal *amoA* gene was amplified using the barcoded primers Arch-amoAF (5'-adaptor+barcode+GAT+STAATGGTCTGGCTTAGACG-3') and Arch-amoAR (5'-adaptor+barcode+GAT+GCGGCCATCCATCTGTATGT-3') (Francis et al. 2005). Triplicated PCR reactions were performed in 12.5 μl mixture contained 1×PCR buffer, 2 mM $MgCl_2$, 0.2 mM dNTP mix, 0.4 μM of respective primers, and 2 U Invitrogen Platinum Taq DNA polymerase (Life Technologies, Carlsbad, CA, USA) and 1 μl template. The PCR thermal cycle consisted of 5 min initial denaturation at 95 ℃ and followed by 33 cycles of 95 ℃ for 30s, 53 ℃ for 45s, and 72 ℃ for 60s and 10 min of final extension step at 72 ℃. The triplicated PCR products of each sample were pooled together and sequenced on the Ion GeneStudio S5 system (Thermo Fisher Scientific, USA) which could generate around 600 bp high quality reads.

2.5 Standard curve construction and Quantitative PCR

The *amoA* gene of AOA and β-AOB *amoA* was amplified by the primer pair Arch-amoAF-amoAR (Francis et al. 2005) and amoA-1F and amo-2R (Rotthauwe et al. 1997) respectively, using the DNA mixture from A-transect samples. The PCR products were purified using the illustra GFX PCR DNA and Gel band purification kit (GE Healthcare, UK) and ligated into T-vector pMD 19 at 4 ℃ for 12 h (Takara, Japan). The ligated vectors solution was mixed with freshly prepared *E. coli* BL21 competent cell and incubated on ice for 30 min. Heat-shock treatment at 42 ℃ were performed for the mixture for 90 s and incubated on ice for 5 min. After 5min incubation, 200 μl of liquid lysogeny broth was added and incubated at 37 ℃ for 1h in incubator shaker (250 rpm/min). The culture was soon spread on to ampicillin (100 $mg \cdot L^{-1}$) plates and incubated at 37 ℃ for 12 h. White clone was selected and confirmed with respective PCR amplification. The clones were expended with ampicillin (100 $mg \cdot L^{-1}$) lysogeny broth sent for sequencing in BGI Tech (BGI, Shenzhen, China). The sequence of the selected plasmid was confirmed as an archaeal *amoA* gene by blast against the NCBI database. The plasmid of the selected clone was extracted and purified by the TIANprep Mini Plasmid Kit (TIANGEN, China). The extracted plasmid was linearized by EcoRI (New England Biolabs) at 37 ℃ for 12 h and purified by electrophoresis on 1.2 % agarose gel. The linearized plasmid DNA concentration was determined via dsDNA HS assay on the Qubit fluorometer v3.0 (Thermo Fisher Scientific, Singapore). Series dilution of the linearized plasmids was amplified as standard curves together with the field samples on the 384-well plates on Roche LightCycler 480.

Triplicated PCR was performed in 10 μl mixture contained 1 × LightCycler® 480 SYBR® Green I Master, 0.5 μM primers pairs and DNA templates. The thermal cycler of the quantitative PCR consisted of a 5 min denaturation at 95 ℃, followed by 45 cycles each at 95 ℃ for 30s, 53 ℃ (60 ℃ for β-AOB) for 45s, 72 ℃ for 60s with single signal acquisition at the end of each cycle. Amplification specificity was confirmed via the melting curve and gel electrophoresis. Both particle attached (> 3 μm) and free-living (0.2-3 μm) from DNA and RNA (using cDNA as a template) ammonia-oxidizing archaea and

https://doi.org/10.5194/bg-2020-223
Preprint. Discussion started: 3 July 2020

ammonia-oxidizing β-proteobacteria abundance were quantified based on the *amoA* gene abundance through quantitative polymerase chain reaction (Table S2).

2.6 Bioinformatic analysis

In total, 76 sample sequencing data (contained 2523 reads per file) files were quality control and analyzed using the microbial ecology community software program Mothur (Schloss et al. 2009). The sequencing output was split according to corresponding barcode sequences in the forward primer. Quality control was performed by discarding reads with low-quality (average quality score < 20), or reads with incorrect length (no shorter than 300 bp and no longer than 630 bp), or reads containing any ambiguous base, or reads containing homopolymers longer than 8 bp. The chimeric sequences were identified and discarded by the *Chimera.uchime* in Mothur package. The archaeal *amoA* sequence through alignment of the *amoA* sequence from the NCBI database (Agarwala et al. 2018). The remaining high-quality sequences were clustered into operational taxonomic units (OTUs) at 95 % similarity. The singletons and doubletons were discarded from the OTUs table before downstream analysis. The representative sequences of the top OTUs were randomly selected through *getotu.rep* in Mothur and blast against the NCBI database (the top OTUs were selected based on relative abundance ≥ 0.1 % (Logares et al. 2014). The Maximum Likelihood phylogenetic tree was constructed in Mega 7 with the recommended model (T92+G+I) after the best model selection. The ML-tree were further edited with iTOL (Letunic and Bork 2016).

Spearman correlation analysis was performed by separating the AOA community retrieved from Surface DNA; Surface RNA; Bottom DNA, Bottom RNA, and corresponding environmental factors, respectively, regarding strong stratification and steep variation of environmental factors that associated with the freshwater discharge in the PRE. Spearman correlation analysis was performed between nitrification rates and *amoA* gene (AOA and β-AOB) abundance retrieved from particle attached (> 3 μm) and free-living (3-0.2 μm) samples.

3 Results

3.1 Hydrographic characteristics of Pearl River estuary

The Pearl River estuary consists of three major sub-estuaries, namely Lingdingyang, Modaomen, and Huangmaohai (Fig. 1), which contributed to the annual mean of freshwater discharge by 55 %, 28 %, and 13 %, respectively (Zhao 1990). The observation was conducted in the wet season when the freshwater discharged into Pearl River estuary can reach 80 % of the annual river discharge (Zhao 1990). The studied area covered a full range of salinity from 0.1 to 34.7, and a huge freshwater plume extended southwestward (Fig. 2a). Associated with the plume area, excessive phytoplankton bloom was observed in the lower estuary with chlorophyll-a concentration peak (28.4 $\mu g \cdot L^{-1}$) at station F202 (Fig. 2b). Furthermore, wide-spread bottom hypoxia (DO < 2 $mg \cdot L^{-1}$) was observed in the lower reach of Pearl River estuary extending from Huangmaohai to the southern water of Hong Kong island (Fig. 2f). The spatial pattern of nitrate concentration was associated with that of salinity (Fig. 2c). The high concentration of nitrate was detected in low salinity water near the outlet of sub-estuaries, and the nitrate

https://doi.org/10.5194/bg-2020-223
Preprint. Discussion started: 3 July 2020


Biogeosciences Discussions Open Access EGU

concentration (over 115 μmol·L^{-1}) peaked in the surface water of Lingdingyang (station A01-03). Similar to nitrate, the nitrite concentration at surface layer was also higher near the estuary outlets and peaked in station A01 with 9.5 μmol·L^{-1}, while in the bottom layer, nitrite displayed relatively constant concentration (< 2 μmol·L^{-1}), spreading southeastward (Fig. 2e). The ammonium concentration displayed a different spatial pattern compared to nitrate and nitrite, which was probably because of local sewage discharges. The ammonium concentration peaked at A06 at both surface and bottom layer with 2.5 μmol·L^{-1} and 3.2 μmol·L^{-1} respectively during the cruise period. A patch of ammonium replete water (over 1 μmol·L^{-1}) was observed in the southern water of Hong Kong, spreading eastward at the stations along the south border-line of Hong Kong water (Fig. 2d).

3.2 The spatial pattern of nitrification rates and their oxygen consumption

The nitrification rate was generally higher in bottom water than in surface water, except station A01 and F601 (Fig. 3). At the surface layer, a high nitrification rate was detected in the outlet of Humen and Modaomen (station A01 and F301) and the southern water of Hong Kong (F601 and F701). At the bottom layer, a high nitrification rate was detected in the Humen outlet and the lower estuary from Huangmaohai to the southern water of Hong Kong (Fig. 3). The oxygen demand of nitrification (NOD) ranged from 0.0001 to 0.1376 mg O_2·L^{-1}·d^{-1} (Fig. 3). The community respiration rate (total oxygen consumption rate, CR) was higher at the surface layer than the corresponding bottom layer in all stations (Fig. 3, Table S3). The community respiration rate at surface layer ranged from 0.22 to 1.68 mg O_2·L^{-1}·d^{-1}, and that at bottom layer ranged from 0.002 to 0.82 mg O_2·L^{-1}·d^{-1}. Based on the ratio between NOD and CR, nitrification contributed 0.01-22.45 % and 0.01-229.21 % of total oxygen consumption at the surface and bottom layer, respectively (Fig. 3). It is noteworthy that nitrification contributed substantially to the total oxygen consumption in the upper estuary and bottom hypoxic water. For the upper estuary in Lingdingyang, nitrification potentially contributed 7.78 % and 11.90 % of the total oxygen consumption at station A01 and A05, respectively. As for the bottom hypoxic water, nitrification accounted for 35.45 % at F101, 14.22 % at F301, 10.27 % at F303, 5.44 % at A09, 81.77 % at F305 and 229.21 % at F701 of the total oxygen consumption.

3.3 Spatial patterns of the abundance of AOA and β-AOB

As inferred from the *amoA* gene copy number, AOA showed a 2-3 order magnitude more abundant than β-AOB (Fig. 4). The archaeal *amoA* was more abundant at the bottom layer than at the surface layer (Fig. 5). The abundance of archaeal *amoA* ranged from 6.27×10^4 to 3.63×10^7 copy·L^{-1} at surface layer and 3.59×10^5 to 4.98×10^8 copy·L^{-1} at the bottom layer, in which the abundance peaked at the bottom layer of station F405. The archaeal *amoA* abundance showed a general decreasing trend from the upper estuary to the continental shelf at the surface layer (Fig. 5). It is noteworthy that archaeal *amoA* was highly abundant in the hypoxic water located in the lower reach of the estuary. The abundance of β-proteobacteria *amoA* at surface layer ranged from 2.03×10^2 to 1.07×10^5 copy·L^{-1}, while at the bottom layer, the abundance of β-proteobacteria *amoA* ranged from 1.91×10^3 to 2.44×10^5 copy·L^{-1} (Fig. 5). The β-proteobacteria *amoA* abundance peaked

https://doi.org/10.5194/bg-2020-223
Preprint. Discussion started: 3 July 2020


Biogeosciences Discussions Open Access EGU

at the surface layer of station A01 in the upper estuary of Lingdingyang with 1.07×10^5 copy·L^{-1} while the lowest abundance detected at the surface layer of station A12 with 2.03×10^2 copy·L^{-1}. The spatial pattern of β-proteobacteria *amoA* at the surface layer was more abundant at the upper estuary of Lingdingyang at A01&A05 and F303 at Modaomen, while the abundance decreased seaward at the bottom layer. Overall, the AOA showed higher abundance in the free-living fraction while AOB was more abundant in the particle attached fraction (Fig. 5, Table S2). Quantification of *amoA* from cDNA (template for RNA level from 13 selected stations) showed archaeal *amoA* ranged from 6.03×10^2 to 3.21×10^6 copy·L^{-1} while β-proteobacteria *amoA* were under detection limit (Table S4). Nitrification rates showed a moderate correlation with the total abundance of β-AOB (r_s= 0.38, $P < 0.05$) at DNA level. Nitrification rates displayed moderate positive correlation with the abundance of AOA (r_s= 0.38, $P < 0.05$) and β-AOB (r_s= 0.33, $P < 0.05$) at particle attached fraction, respectively.

3.4 Phylogenetic diversity of AOA

Given that the AOA is the dominant ammonia oxidizer throughout the estuary, we further investigate the phylogenetic diversity of AOA at DNA and RNA level in 13 stations covering from the upper estuarine to oceanic environments. In total, 191,748 high-quality *amoA* sequences were retrieved from 76 samples in the 13 station (Table S5) and operational taxonomic units (OTUs) were detected at 95 % DNA similarity after removal of singletons and doubletons. Top OTUs (OTUs with mean relative abundance ≥ 0.1 % among samples) were focused in this study. The Maximum likelihood (ML) phylogenetic tree showed that the top 85 OTUs (OTUs with mean relative abundance ≥ 0.1 % among samples) affiliated to WCA sublineages and SCM1-like clade according to the reference sequence in Jing et al. 2017 and Cheung et al. 2019 (Cheung et al. 2019; Jing et al. 2017). Half of the top OTUs were affiliated to the two WCA sublineages, WCA I (13 OTUs) and WCA II (32 OTUs). Besides, diverse phylotypes OTUs that affiliated to SCM1-like clade, which showed > 90 % DNA similarity with the *amoA* sequences of *Nitrosopumilis maritimus* SCM1, were recovered. These SCM1-like OTUs were grouped into four sublineages according to the topology of the ML tree, includes SCM1-like-I (10 OTUs), SCM1-like-II (16 OTUs), SCM1-like-III (6 OTUs) and SCM-like-IV clade (8 OTUs) (Fig. 6). The SCM1-like III were phylogenetical close to *Nitrosoarchaeum limnia* (Fig. 6 and S2)

3.5 Differential distribution of AOA sublineages at DNA and RNA level

As revealed by the Non-metric multidimensional scaling (NMDS) analysis, a strong dissimilarity between DNA and RNA communities were observed (Fig. 7). On the other hand, different AOA sublineages showed distinct distributional patterns (Fig. 6 and 8). WCA I was mainly distributed in bottom layers except for the upper reach of Lingdingyang. At the surface layer, the WCA I was generally minor in the AOA community, while it was dominant occasionally in the plume area with median salinity. At RNA level, WCA I showed lower abundance at median salinity at the surface layer and showed increasing relative abundance seaward (Fig. 6 and 8).

https://doi.org/10.5194/bg-2020-223
Preprint. Discussion started: 3 July 2020

The AOA community at DNA level was dominated by WCA II which showed ubiquitous distribution for salinity 0.1-34.5. Exceptionally, WCA II was outnumbered by SCM1-like-III at the surface layer at station F301 near the Modaomen and Huangmaohai which is close to freshwater discharge. At RNA level, WCA II showed similar distributional patterns and relative abundance with WCA I; and contributed an increasing proportion of the active AOA community from the upper estuary to the continental shelf (Fig. 6 and 8).

SCM1-like-I mainly distributed at the lower reach of the estuary; and SCM1-like-I and II were outnumbered by other AOA phylotypes at DNA level. Among SCM1-like sublineages, the SCM1-like-III was the most abundant at DNA level. Their distribution was limited to surface water of the Pearl River and freshwater plume (salinity < 14) (Fig. 6 and 8). However, the SCM1-like sublineages were surprisingly dominating the active AOA communities at RNA level. The SCM1-like-II dominated the active AOA communities in the Pearl River and its lower reach at the bottom layer, while at the surface layer, the SCM1-like-IV was showed high relative abundance at RNA level (Fig. 8). Besides, the SCM1-like-I was less abundant than SCM1-like-II at RNA level at the bottom layer, and its spatial pattern was similar to SCM1-like-II. In addition, SCM1-like-III was the least abundant among the SCM1-like sublineages at RNA level. The distribution of SCM1-like-III at RNA level was still limited to the freshwater regions (Fig. 6) similar to its spatial pattern showed at DNA level.

3.6 Correlation between AOA sublineages and environmental factors

To reveal the connections between genetic diversity of AOA sublineages and environmental factors, the correlation between different sublineages and environmental factors were examined using Spearman correlation coefficients. The AOA communities were separated into 4 parts: surface DNA; surface RNA, bottom DNA; bottom RNA level, and analyzed with the corresponding environmental factors. Generally, the relative abundance of AOA sublineages showed a more significant correlation with environmental factors both at DNA and RNA levels at the bottom layer (Fig. 9). Among 9 environmental factors, salinity showed the most significant correlation with AOA sublineage distribution.

WCA sublineages showed a strong positive correlation with salinity while SCM1-like sublineages showed a negative correlation with salinity. At RNA level in the bottom layer, SCM1-like-I and IV were positively correlated with nutrient concentration and heterotrophic bacteria abundance while negatively correlated with salinity and dissolved oxygen concentration. SCM1-like-III showed a strong negative correlation with salinity at both surface and bottom layers. Nutrient concentration showed an opposite pattern comparing with salinity which was regarded as an association of nutrients with freshwater discharge. Ammonium, as the substrate for nitrification, showed no significant correlation with AOA sublineage distribution which may be introduced by the large variance of the ammonia concentration in the dynamic estuarine ecosystem.

The Spearman correlation between nitrification rates (NR) and the relative abundance of AOA sublineages was also revealed in Fig. 9. SCM1-like-III showed a positive correlation with nitrification rate at surface water at RNA level, while SCM1-like-I (r_s= 0.81, $P < 0.05$) and SCM1-like-IV sublineage (r_s= 0.73, $P < 0.05$) showed a positive correlation with nitrification rates at the bottom layer at RNA level. Besides, WCA I showed a positive correlation with nitrification rates (r_s=

https://doi.org/10.5194/bg-2020-223
Preprint. Discussion started: 3 July 2020

0.75, $P < 0.05$) only at the surface layer at RNA level While WCA II showed a negative correlation (r_s= -0.73, $P < 0.05$) with nitrification rates at the bottom layer.

4 Discussion

4.1 Nitrification and its oxygen consumption in the hypoxia zone

We observed wide-spread hypoxia-zone at the lower estuary of Pearl River, extending from Huangmaohai to South of Hong Kong which was in favor by both physical and biogeochemical conditions (Fig. 2-F). During the 2017 summer cruise, we observed intensive river discharge inferred from salinity at the surface layer (Fig. 2-A), which is the typical wet season pattern of Pearl River estuary (Harrison et al. 2008). The continuous river discharge sustained strong stratification at the lower estuary which blocked the air-sea oxygen exchange to the bottom water. Furthermore, a high concentration of nutrients associated with the freshwater from three sub-estuaries sustained high phytoplankton biomass in the lower reach of the estuary (Fig. 2-B). The massive locally generated and riverine organic matter sunk down to the bottom layer and rapidly degraded by bacteria, leading to high oxygen consumption (Harrison et al. 2008; Lu et al. 2018).

In the Pearl River estuary, we found nitrification could contribute a large proportion of oxygen consumption in the hypoxia zone in which nitrification potentially accounted for 35.35 % at F101, 14.22 % at F301, 10.27 % at F303, 5.14% at A09 and 81.77 % at F305 and 229.21 % at F701. In the eutrophic Delaware River estuary, nitrification accounted for over 20 % of the oxygen consumption river downstream (Lipschultz et al. 1986). Intensive nitrification was observed at intermediate salinities which accounted for 20 to over 50 % of oxygen consumption. (Pakulski et al. 1995). It has been reported that nitrification could contribute to one-third of total oxygen consumption in the upper (from Guangzhou to Humen) Pearl River estuary (Dai et al. 2008) which suggested active nitrification could substantially draw down oxygen concentration leading to hypoxia formation. Respiration and nitrification are both important and coupled oxygen-consuming processes. It is well-known that ammonia, the substrate of nitrification, was produced during the organic matter degradation (respiration). Thus, nitrification was not only supported by riverine ammonia but also supported by rapid organic matter degradation in the Pearl River estuary. We observed the high nitrification rate associated with the upper estuary and the hypoxia zone (Fig. 3) where the corresponding community respiration rates were high as well in the bottom layer. Comparing with the community respiration, we found that nitrification substantially contributed to total oxygen consumption at the bottom layer by 15.30 % (excluding 229.21 % from F701) on average (ranged from 0.01 to 229.21 %). We found one data of NOD exceeding CR from our entire cruise observed at F701. In 2014 in Changjiang estuary, Hsiao et al. also found the potential nitrification oxygen consumption exceeded the total oxygen consumption and speculated the other oxidants (Fe and Mn) could potentially oxidized ammonia (Hsiao et al. 2014). Oxygen might be considered as limiting factors to nitrifying activity as oxygen concentration were much lower under hypoxic condition (< 2mg·L^{-1}). However, nitrification remained active under nanomolar range of oxygen (< 10 nM) (Bristow et al. 2016). During the cruise, the lowest oxygen concentration is 0.54 mg·L^{-1} (16.88 μM) that the oxygen concentration was not limiting for nitrification activities (Bristow et

https://doi.org/10.5194/bg-2020-223
Preprint. Discussion started: 3 July 2020

al. 2016). Hence, in the Pearl River Estuary, nitrification could substantially draw down oxygen concentration favored by physicochemical and biogeochemical conditions, sustaining hypoxia formation at the lower estuary.

4.2 Relative distribution of AOA and AOB in Pearl River Estuary

Both AOA and AOB present in the estuarine environment, however, their contribution to the nitrification activities remained under exploration. The abundance of the AOA and AOB in the pelagic ocean has been well identified with AOA outnumber AOB by orders of magnitude while in the estuarine environment, the ratio of AOA and AOB were rather variable. Estimated based on quantitative PCR (qPCR) of *amoA* gene, AOB were relatively more abundant than AOA the in many coastal and estuarine sediments (Caffrey et al. 2007; Mosier and Francis 2008; Santoro et al. 2008; Magalhaes et al. 2009; Wankel et al. 2011) while AOA were orders of magnitude more abundant than AOB in other estuaries and coastal environment (Caffrey et al. 2007; Moin et al. 2009; Abell et al. 2010; Bernhard et al. 2010; Mosier and Francis 2011). The variance and relative distribution of AOA and AOB as well as the nitrification rates have been shown related to various physicochemical parameters such as salinity, dissolved oxygen, ammonia, pH, etc. in the various estuarine environment (Bernhard and Bollmann 2010; Mosier and Francis 2011). Comparing to the previous estuarine studies based on DNA survey, we conduct a comprehensive quantification of AOA and β-AOB abundance at both DNA and RNA levels as well as the nitrification rates in the Pearl River estuary. In Pearl River estuary, AOA outnumbers AOB throughout the estuarine at DNA level. Furthermore, AOA was detectable in RNA level while AOB was lower than the detection limit which suggested AOA were the active ammonia oxidizers in the Pearl River estuary. Though size-fractionated nitrifiers abundance, the differential distribution of these two group ammonia oxidizers were observed. We found AOA mainly distributed in the free-living fraction while AOB associated with the particles near upper estuary which may be explained by higher substrate requirement of AOB than AOA (Martens-Habbena et al. 2009).

4.3 Unneglectable disagreement of the AOA community at DNA and RNA level

In our study, the positive correlations between nitrification rates and different AOA sublineages suggested the divergence of nitrification activities among the AOA population in the dynamic estuarine ecosystems (Fig. 9). Given that AOA plays a central role in the nitrogen cycle, the physiological characteristics of the highly diverse AOA are an essential basis for understanding the nitrogen cycle in the current and future ocean. With the limitation of underrepresented cultures and genomes, numerous AOA related studies in the ocean were based on amplicon sequencing and qPCR targeting archaeal *amoA* (Beman et al. 2008; Bernhard and Bollmann 2010; Peng et al. 2013; Santoro et al. 2017; Alves et al. 2018). However, it should be noted that almost all these studies were based on DNA samples. In our study, the obvious disagreement between the AOA communities at DNA and RNA levels (Fig. 8) indicated that different AOA sublineages may have functional differences. Coincidentally, a similar phenomenon has also been recently reported in the terrestrial ecosystem, in which *Nitrososphaera* and its sister group were more active than *Nitrosotalea* in acidic forest soils (Wu et al. 2017). As reported in a previous study in the Pacific Ocean, the *amoA* abundance of WCA and WCB have no correlation with nitrification rates

https://doi.org/10.5194/bg-2020-223
Preprint. Discussion started: 3 July 2020

throughout the water column indicated the active functional group of AOA might be neglected at DNA based study (Smith et al. 2016). In the light of our finding, the abundant AOA sublineages (WCA) can be much less active ammonia oxidizers than the rare sublineages (SCM1-like) (Fig. 7 and 8), which suggested that the DNA-based observations were insufficient to unravel the major ammonia oxidizer in the ocean. Furthermore, given that highly diverse sublineages of WCA and WCB have recently been reported in the oceanic waters (Cheung et al. 2019; Lu et al. 2019), the nitrification activity of different AOA sublineages should be further verified in the future field studies.

4.4 AOA sublineages and their potential niche in the estuarine ecosystem

The ammonia-oxidizing archaea in the estuarine water were less studied compared to the populations from estuarine sediments, oceanic waters, and soils since the discovery of AOA (Damashek et al. 2016). In the sediment from San Francisco Bay, Mosier and Francis (2008) had proposed a cluster of AOA phylotypes potentially adapted to a low salinity environment (Mosier and Francis 2008). However, these phylotypes were then also observed in a salt marsh (Moin et al. 2009) which leads to questionable low-salinity adaption assumption (Bernhard and Bollmann 2010). On the other hand, exploration of diversity and biogeography of different AOA were limited by low-coverage clone library method as well as neglected active population at RNA level. Furthermore, in most cases, relatively weak or no correlation between nitrification rates and archaeal *amoA* gene abundance (Bernhard and Bollmann 2010) indicated the physiological differences of ammonia oxidizers. The above-mentioned scenario indicated that it is necessary to study key and active ammonia oxidizers among the population to understand their contribution in nitrification activities in the field.

In our study, we found the differential niche partitioning of AOA sublineages in the dynamic PRE ecosystem in which the AOA community mainly consisted of WCA and SCM1-like sublineages, while WCB were not detected. This pattern was consistent with the previous studies that WCA and SCM1-like mainly distributed in surface water and WCB was limited to deep mesopelagic waters (Francis et al. 2005; Beman et al. 2008). In a recent study based on the Tara *Oceans* dataset, WCA I dominated the surface water AOA communities throughout the global oceans (Cheung et al. 2019). In this study, WCA I was generally minor in the estuary except for the high salinity bottom water that intruded from the South China Sea (Fig. 8), which indicated that WCA I prefers the conditions of oceanic waters. As revealed by the genomic and proteomic of its representative culture (*Candidatus Nitrosopelagicus brevis* CN25), the WCA I have a streamlined genome with high coding density and ubiquitously distributed oligotrophic surface ocean (Santoro et al. 2015). In contrast, WCA II was dominant in the AOA communities throughout the studied region at DNA level (Fig. 8), which agree with the previous study that its relative abundance was generally higher in marginal seas (the Gulf of Mexico, the Red Sea, and the Arabian Sea) than in oceanic waters (Cheung et al. 2019). The present study showed that WCA II outnumbered WCA I in the estuarine ecosystem, which strongly indicated the niche partition between WCA I (oceanic water preferred) and WCA II (coastal water preferred). Nevertheless, these two WCA sublineages only contributed a small portion of the archaeal *amoA* gene transcripts and did not show a significant correlation with nitrification rate (Fig. 9), which indicated that they were not the major ammonia oxidizers

https://doi.org/10.5194/bg-2020-223
Preprint. Discussion started: 3 July 2020

in the estuarine ecosystem. Hence, the ecological function of these abundant WCA sublineages in the estuarine ecosystem should be further explored in future studies.

Regarding the active population in RNA level, highly diverse SCM1-like OTUs were recovered in this study, which was highly similar to the *amoA* gene of *Nitrosopumilus maritimus* SCM-1 (Fig. 6) (Konneke et al. 2005). In particular, the 4 SCM1-like sublineages defined in this study displayed distinct distributional patterns: SCM1-like-I and II mainly distributed in the lower reach of the river; SCM1-like-IV was mainly active at the surface layer in the estuary; SCM1-like-III was limited to freshwater, implied distinct niche partitioning of the SCM1-like sublineages (Fig. 8). As inferred from RNA communities and correlation analysis result, SCM1-like-I was the major active ammonia oxidizer in the PRE water column. The earlier view presumed that the AOA are chemolithoautotrophs that largely rely on ammonia oxidation for energy acquisition. However, increasing evidence suggested that marine AOA (i.e. *N. maritimus* strains) can utilize organic nitrogen (i.e. urea and cyanate) as the substrates of nitrification, or utilize organic nutrient (Qin et al. 2014; Kitzinger et al. 2019). Hence, it may explain that the high nitrification activities of the SCM1-like sublineages were facilitated by the enriched and diverse nitrogen sources in estuarine water. Recent culture-based studies found the physiology of *N. maritimus* was not significantly influenced by salinity changes in the growth medium (Elling et al. 2015, Qian et al. 2015) which indicated SCM1-like can tolerant to wide salinity range. Furthermore, SCM1-like-I showed a positive correlation with heterotrophic bacteria abundance at RNA level together with a high abundance of AOA and heterotrophic bacteria in the hypoxic zone, indicating potential interaction between organic matter degradation and nitrification activities. On the other hand, SCM1-like-I and II were the major ammonia oxidizers in the hypoxic waters (Fig. 9), where nitrification contributed significantly to the total oxygen consumption (Fig. 4). Consistently, *N. maritimus* was actively nitrifying and grew under low oxygen conditions (Qin et al. 2017).

The spatial distribution of SCM1-like-III as well as the negative correlation with salinity indicated the SCM1-like-III is associated with freshwater discharge. The SCM1-like-III was closely related to the *amoA* gene fragment of *Nitrosoarchaeum limnia* which was a low-salinity adapted species (Fig. S2). The functional potential of low-salinity adaptation of *N. limnia* was further evidenced by genomic information from enrichment culture (estuarine sediment from San Francisco Bay) (Blainey et al. 2011). The genome of *N. limnia* SFB1 possessed numerous motility- and chemotaxis-associated genes that might facilitate their adaptation to the fluctuating estuarine environment (Blainey et al. 2011). Further genomic and metabolic studies were needed to understand the ecological role of SCM1-like-III in the freshwater discharge. In summary, our study provides the first evidence of the niche partition and different activities of different AOA sublineages in estuarine water, suggesting that more efforts are needed for a comprehensive understanding of the ecological role of AOA in various ecosystems.

https://doi.org/10.5194/bg-2020-223
Preprint. Discussion started: 3 July 2020

5 Data availability

The *amoA* gene abundance at DNA level from 23 station along with nitrification rates were listed in Table S2. Nitrification and community respiration and nitrification oxygen demand were listed in Table S3. The *amoA* abundance at RNA (cDNA) level from 13 stations were listed in Table S4. The complete sequencing dataset was available at NCBI under the Bioproject number PRJNA610708. Data will be released once the paper is published. The information of the sequencing samples was listed in Table S5.

6 Author Contributions:

HBL conceived the project. YHL performed experiments, analyzed and interpreted the data. YHL and SYC wrote the manuscript. XMX edited the manuscript. LC and SJK provided nitrification rates data. JPG provided physical profiles of the project. MHD provided nutrient and dissolved oxygen profiles of the project. All the authors provided critical feedback and help shape the research, analysis and manuscript.

7 Competing interests:

The authors declare that they have no conflict of interest.

8 Acknowledgments

This work was supported by the Research Grants Council (Hong Kong RGC) Theme-Based Research Scheme (T21-602/16-R), the RGC-NSFC Joint Research Scheme (N_HKUST609/15), and the GRF grants (16128416, 16101318). This study was also supported by the Hong Kong Branch of Southern Marine Science & Engineering Guangdong Laboratory.

9 References

Abell, G. C. J., A. T. Revill, C. Smith, A. P. Bissett, J. K. Volkman, and Robert, S. S. : Archaeal ammonia oxidizers and *nirS*-type denitrifiers dominate sediment nitrifying and denitrifying populations in a subtropical macrotidal estuary, ISME J., 4, 286–300, https://doi.org/10.1038/ismej.2009.105, 2010.

Agarwala, R. Barrett, T. Beck, J. Benson, D. A. Bollin, C. Bolton, E. Bourexis, D. Brister, J. R. Bryant, S. H. Canese, K. Cavanaugh, M. Charowhas, C. Clark, K. Dondoshansky, I. Feolo, M. Fitzpatrick, L. Funk, K. Geer, L. Y. Gorelenkov, V. Graeff, A. Hlavina, W. Holmes, B. Johnson, M. Kattman, B. Khotomlianski, V. Kimchi, A. Kimelman, M. Kimura, M. Kitts,

430 P. Klimke, W. Kotliarov, A. Krasnov, S. Kuznetsov, A. Landrum, M. J. Landsman, D. Lathrop, S. Lee, J. M. Leubsdorf, C.
431 Lu, Z. Y. Madden, T. L. Marchler-Bauer, A. Malheiro, A. Meric, P. Karsch-Mizrachi, I. Mnev, A. Murphy, T. Orris, R.
432 Ostell, J. O'Sullivan, C. Palanigobu, V. Panchenko, A. R. Phan, L. Pierov, B. Pruitt, K. D. Rodarmer, K. Sayers, E. W.
433 Schneider, V. Schoch, C. L. Schuler, G. D. Sherry, S. T. Siyan, K. Soboleva, A. Soussov, V. Starchenko, G. Tatusova, T. A.
434 Thibaud-Nissen, F. Todorov, K. Trawick, B. W. Vakatov, D. Ward, M. Yaschenko, E. Zasypkin, A. and Zbicz, K. : Database
435 resources of the National Center for Biotechnology Information, Nucleic Acids Res. 46**:** D8–D13.
436 https://doi.org/10.1093/nar/gkx1095, 2018.

437 Alves, R. J. E., B. Q. Minh, T. Urich, A. von Haeseler, and Schleper, C. : Unifying the global phylogeny and environmental
438 distribution of ammonia-oxidising archaea based on *amoA* genes. Nat. Commun., 9, https://doi.org/10.1038/s41467-018-
439 03861-1, 2018.

440 Beman, J. M., B. N. Popp, and Alford, S. E. : Quantification of ammonia oxidation rates and ammonia-oxidizing archaea and
441 bacteria at high resolution in the Gulf of California and eastern tropical North Pacific Ocean, Limnol. Oceanogr., 57, 711–
442 726, https://doi.org/10.4319/lo.2012.57.3.0711, 2012.

443 Beman, J. M., B. N. Popp, and Francis, C. A. : Molecular and biogeochemical evidence for ammonia oxidation by marine
444 Crenarchaeota in the Gulf of California, ISME J., 2, 429–441, https://doi.org/10.1038/ismej.2007.118, 2008.

445 Bernhard, A. E., and Bollmann, A. : Estuarine nitrifiers: New players, patterns and processes, Estuar. Coast. Shelf Sci. 88, 1–
446 11, https://doi.org/10.1016/j.ecss.2010.01.023, 2010.

447 Bernhard, A. E., Z. C. Landry, A. Blevins, J. R. de la Torre, A. E. Giblin, and Stahl, D. A. : Abundance of ammonia-
448 oxidizing archaea and bacteria along an estuarine salinity gradient in relation to potential nitrification rates, Appl. Environ.
449 Microbiol. 76, 1285–1289, https://doi.org/10.1128/Aem.02018-09, 2010.

450 Blainey, P. C., A. C. Mosier, A. Potanina, C. A. Francis, and Quake, S. R. : Genome of a Low-salinity ammonia-oxidizing
451 archaeon determined by single-cell and metagenomic analysis, PLoS One, 6, https://doi.org/10.1371/journal.pone.0016626,
452 2011.

453 Bristow, L. A. Dalsgaard, T. Tiano, L. Mills, D. B. Bertagnolli, A. D. Wright, J. J. Hallam, S. J. Ulloa, O. Canfield, D. E.
454 Revsbech, N. P. Thamdrup, B. : Ammonium and nitrite oxidation at nanomolar oxygen concentrations in oxygen minimum
455 zone waters, Proc. Natl. Acad. Sci. USA 113, 10601–10606, https://doi.org/10.1073/pnas.1600359113, 2016.

456 Caffrey, J. M., N. Bano, K. Kalanetra, and Hollibaugh, J. T. : Ammonia oxidation and ammonia-oxidizing bacteria and
457 archaea from estuaries with differing histories of hypoxia, ISME J., 1, 660–662, https://doi.org/10.1038/ismej.2007.79, 2007.

458 Campbell, L. G., J. C. Thrash, N. N. Rabalais, and Mason, O. U. : Extent of the annual Gulf of Mexico hypoxic zone
459 influences microbial community structure, PLoS One, 14, https://doi.org/10.1371/journal.pone.0209055, 2019.

460 Casciotti, K. L., D. M. Sigman, M. G. Hastings, J. K. Bohlke, and Hilkert, A. : Measurement of the oxygen isotopic
461 composition of nitrate in seawater and freshwater using the denitrifier method., Anal. Chem., 74, 4905–4912,
462 https://doi.org/10.1021/ac020113w, 2002.

463 Chen, L., Zhang, X., Lai, Y., Liu, J., Lu, Y. H., Liu, H. B., Dai, M. H., Gan, J. P. and Kao, S. J. : Dark ammonium
464 transformations in the Pearl River Estuary during summer (in review)

465 Cheung, S., W. Mak, X. M. Xia, Y. H. Lu, Y. Y. Cheung, and Liu, H. B. : Overlooked genetic diversity of ammonia
466 oxidizing archaea lineages in the global oceans., J. Geophys. Res. Biogeo., 124, 1799–1811,
467 https://doi.org/10.1029/2018jg004636, 2019.

468 D. Kahle and Wickham, H. : ggmap: Spatial Visualization with ggplot2. The R J., 51, 144-161, URL http://journal.r-
469 project.org/archive/2013-1/kahle-wickham.pdf, 2013.

470 Dai, M. H. Guo, X. G. Zhai, W. D. Yuan, L. Y. Wang, B. W. Wang, L. F. Cai, P. H. Tang, T. T. and Cai, W. J. : Oxygen
471 depletion in the upper reach of the Pearl River estuary during a winter drought, Mar. Chem., 102, 159–169,
472 https://doi.org/10.1016/j.marchem.2005.09.020, 2006.

473 Dai, M. Wang, L. Guo, X. Zhai, W. Li, Q. He, B. and Kao, S. J. : Nitrification and inorganic nitrogen distribution in a large
474 perturbed river/estuarine system: the Pearl River Estuary, China, Biogeosciences, 5, 1227–1244. https://doi.org/10.5194/bg-
475 5-1227-2008, 2008.

476 Damashek, J., K. L. Casciotti, and Francis, C. A. : Variable nitrification rates across environmental gradients in turbid,
477 nutrient-rich estuary waters of San Francisco Bay, Estuar. Coast., 39, 1050–1071, https://doi.org/10.1007/s12237-016-0071-
478 7, 2016.

479 Elling, F. J., M. Konneke, M. Mussmann, A. Greve, and Hinrichs,K. U. : Influence of temperature, pH, and salinity on
480 membrane lipid composition and TEX86 of marine planktonic thaumarchaeal isolates, Geochim. Cosmochim. Ac., 171,
481 238–255, https://doi.org/10.1016/j.gca.2015.09.004, 2015.

482 Erguder, T. H., N. Boon, L. Wittebolle, M. Marzorati, and Verstraete, W. : Environmental factors shaping the ecological
483 niches of ammonia-oxidizing archaea, FEMS Microbiol Rev., 33, 855–869, https://doi.org/10.1111/j.1574-
484 6976.2009.00179.x, 2009.

485 Francis, C. A., K. J. Roberts, J. M. Beman, A. E. Santoro, and Oakley, B. B. : Ubiquity and diversity of ammonia-oxidizing
486 archaea in water columns and sediments of the ocean, Proc. Natl. Acad. Sci. USA, 102, 14683–14688,
487 https://doi.org/10.1073/pnas.0506625102, 2005.

488 Hallam, S. J. Mincer, T. J. Schleper, C. Preston, C. M. Roberts, K. Richardson, P. M. and DeLong, E. F. : Pathways of
489 carbon assimilation and ammonia oxidation suggested by environmental genomic analyses of marine Crenarchaeota, PLoS
490 Biol., 4, 520–536, https://doi.org/10.1371/journal.pbio.0040095, 2006.

491 Harrison, P. J., K. D. Yin, J. H. W. Lee, J. P. Gan, and Liu, H. B. : Physical-biological coupling in the Pearl River Estuary.
492 Cont. Shelf Res., 28, 1405–1415, https://doi.org/ 10.1016/j.csr.2007.02.011, 2008.

493 Hsiao, S. S. Y. Hsu, T. C. Liu, J. W. Xie, X. Zhang, Y. Lin, J. Wang, H. Yang, J. Y. T. Hsu, S. C. Dai, M. and Kao, S. J. :
494 Nitrification and its oxygen consumption along the turbid Chang Jiang River plume, Biogeosciences, 11, 2083–2098, https://
495 doi.org/10.5194/bg-11-2083-2014, 2014.

496 Jing, H. M., S. Y. Cheung, X. M. Xia, K. Suzuki, J. Nishioka, and Liu, H. B. : Geographic distribution of ammonia-oxidizing
497 archaea along the Kuril Islands in the western subarctic Pacific, Front. Microbiol., 8,
498 https://doi.org/10.3389/fmicb.2017.01247, 2017.

499 Kitzinger, K. Padilla, C. C. Marchant, H. K. Hach, P. F. Herbold, C. W. Kidane, A. T. Konneke, M. Littmann, S.
500 Mooshammer, M. Niggemann, J. Petrov, S. Richter, A. Stewart, F. Wagner, M. Kuypers, M. M. M. and Bristow, L. A. :
501 Cyanate and urea are substrates for nitrification by Thaumarchaeota in the marine environment. Nat. Microbiol., 4, 234–243,
502 https://doi.org/10.1038/s41564-018-0316-2, 2019.

503 Knapp, A. N., D. M. Sigman, and Lipschultz, F. : N isotopic composition of dissolved organic nitrogen and nitrate at the
504 Bermuda Atlantic time-series study site, Global Biogeochem. Cycle, 19, https://doi.org/10.1029/2004gb002320, 2005.

505 Konneke, M., A. E. Bernhard, J. R. de la Torre, C. B. Walker, J. B. Waterbury, and D. A. Stahl. : Isolation of an autotrophic
506 ammonia-oxidizing marine archaeon, Nature 437, 543–546, https://doi.org/10.1038/nature03911, 2005.

507 Letunic, I., and Bork, P. : Interactive tree of life (iTOL) v3: an online tool for the display and annotation of phylogenetic and
508 other trees, Nucleic Acids Res., 44, W242–W245, https://doi.org/10.1093/nar/gkw290, 2016.

509 Lipschultz, F., S. C. Wofsy, and Fox, L. E. : Nitrogen-metabolism of the eutrophic Delaware River ecosystem, Limnol.
510 Oceanogr., 31, 701–716, https://doi.org/10.4319/lo.1986.31.4.0701, 1986.

511 Liu, H. B., H. M. Jing, T. H. C. Wong, and Chen, B. Z. : Co-occurrence of phycocyanin- and phycoerythrin-rich
512 *Synechococcus* in subtropical estuarine and coastal waters of Hong Kong. Environ. Microbiol. Rep., 6, 90–99,
513 https://doi.org/10.1111/1758-2229.12111, 2014.

514 Logares, R. Audic, S. Bass, D. Bittner, L. Boutte, C. Christen, R. Claverie, J. M. Decelle, J. Dolan, J. R. Dunthorn, M.
515 Edvardsen, B. Gobet, A. Kooistra, W. H. C. F. Mahe, F. Not, F. Ogata, H. Pawlowski, J. Pernice, M. C. Romac, S.
516 Shalchian-Tabrizi, K. Simon, N. Stoeck, T. Santini, S. Siano, R. Wincker, P. Zingone, A. Richards, T. A. de Vargas, C. and

517 Massana, R. : Patterns of rare and abundant marine microbial eukaryotes, Curr. Biol., 24, 813–821,
518 https://doi.org/10.1016/j.cub.2014.02.050, 2014.

519 Lu, Y. H., X. M. Xia, S. Y. Cheung, H. M. Jing, and Liu, H. B. : Differential distribution and determinants of ammonia
520 oxidizing archaea sublineages in the oxygen minimum zone off Costa Rica, Microorganisms, 7,
521 https://doi.org/10.3390/microorganisms7100453, 2019.

522 Lu, Z. M., J. P. Gan, M. H. Dai, H. B. Liu, and Zhao, X. Z. : Joint effects of extrinsic biophysical fluxes and intrinsic
523 hydrodynamics on the formation of hypoxia west off the Pearl River Estuary. J. Geophys. Res. Ocean, 123, 6241–6259,
524 https://doi.org/10.1029/2018jc014199, 2018.

525 Magalhaes, C. M., A. Machado, and Bordalo, A. A. : Temporal variability in the abundance of ammonia-oxidizing bacteria
526 vs. archaea in sandy sediments of the Douro River estuary, Portugal, Aquat. Microb. Ecol., 56, 13–23,
527 https://doi.org/10.3354/ame01313, 2009.

528 Martens-Habbena, W., P. M. Berube, H. Urakawa, J. R. de la Torre, and Stahl, D. A. : Ammonia oxidation kinetics
529 determine niche separation of nitrifying Archaea and Bacteria, Nature 461, 976–U234, https://doi.org/10.1038/nature08465,
530 2009.

531 Moin, N. S., K. A. Nelson, A. Bush, and Bernhard, A. E. : Distribution and diversity of archaeal and bacterial ammonia
532 oxidizers in salt marsh sediments, Appl. Environ. Microbiol., 75, 7461–7468, https://doi.org/10.1128/Aem.01001-09, 2009.

533 Mosier, A. C., and Francis, C. A. : Relative abundance and diversity of ammonia-oxidizing archaea and bacteria in the San
534 Francisco Bay estuary, Environ. Microbiol., 10, 3002–3016, https://doi.org/10.1111/j.1462-2920.2008.01764.x, 2008.

535 Mosier, A. C., and Francis C. A. : Determining the distribution of marine and coastal ammonia-oxidizing archaea and
536 bacteria using a quantitative approach, Meth. Enzymol., 486, 205–221, https://doi.org/10.1016/S0076-6879(11)86009-X,
537 2011.

538 Oudot, C., R. Gerard, P. Morin, and Gningue, I. : Precise shipboard determination of dissolved-oxygen (Winkler Procedure)
539 for productivity studies with a commercial system, Limnol. Oceanogr., 33, 146–150,
540 https://doi.org/10.4319/lo.1988.33.1.0146, 1988.

541 Pai, S. C., Y. J. Tsau, and Yang, T. I. : pH and buffering capacity problems involved in the determination of ammonia in
542 saline water using the indophenol blue spectrophotometric method, Anal. Chim. Ac., 434, 209–216,
543 https://doi.org/10.1016/S0003-2670(01)00851-0, 2001.

544 Pakulski, J. D., R. Benner, R. Amon, B. Eadie, and Whitledge, T. : Community metabolism and nutrient cycling in the
545 Mississippi River Plume - Evidence for intense nitrification at intermediate salinities, Mar. Ecol. Prog. Ser., 117, 207–218,
546 https://doi.org/10.3354/meps117207, 1995.

547 Peng, X. F., A. Jayakumar, and Ward, B. B. : Community composition of ammonia-oxidizing archaea from surface and
548 anoxic depths of oceanic oxygen minimum zones, Front. Microbiol., 4, https://doi.org/ 10.3389/fmicb.2013.00177, 2013.

549 Qian, W. Gan, J. P. Liu, J. W. He, B. Y. Lu, Z. M. Guo, X. H. Wang, D. L. Guo, L. G. Huang, T. and Dai, M. H. : Current
550 status of emerging hypoxia in a eutrophic estuary: The lower reach of the Pearl River Estuary, China, Estuar. Coast. Shelf S.,
551 205, 58–67, https://doi.org/10.1016/j.ecss.2018.03.004, 2018.

552 Qin, W. Amin, S. A. Martens-Habbena, W. Walker, C. B. Urakawa, H. Devol, A. H. Ingalls, A. E. Moffett, J. W. Armbrust,
553 E. V. and Stahl, D. A. : Marine ammonia-oxidizing archaeal isolates display obligate mixotrophy and wide ecotypic
554 variation, Proc. Natl. Acad. Sci. USA, 111, 12504–12509. https://doi.org/10.1073/pnas.1324115111, 2014.

555 Qin, W. Carlson, L. T. Armbrust, E. V. Devol, A. H. Moffett, J. W. Stahl, D. A. and Ingalls, A. E. : Confounding effects of
556 oxygen and temperature on the TEX86 signature of marine Thaumarchaeota, Proc. Natl. Acad. Sci. USA, 112, 10979–10984,
557 https://doi.org/10.1073/pnas.1501568112, 2015.

558 Qin, W. Meinhardt, K. A. Moffett, J. W. Devol, A. H. Armbrust, E. V. Ingalls, A. E. and Stahl, D. A. Influence of oxygen
559 availability on the activities of ammonia-oxidizing archaea, Environ. Microbiol. Rep., 9, 250–256,
560 https://doi.org/10.1111/1758-2229.12525, 2017.

561 Reji, L., B. B. Tolar, J. M. Smith, F. P. Chavez, and Francis, C. A. : Differential co-occurrence relationships shaping ecotype
562 diversification within Thaumarchaeota populations in the coastal ocean water column, ISME J., 13, 1144-1158,
563 https://doi.org/10.1038/s41396-018-0311-x, 2019.

564 Rotthauwe, J. H., K. P. Witzel, and Liesack, W. The ammonia monooxygenase structural gene *amoA* as a functional marker:
565 Molecular fine-scale analysis of natural ammonia-oxidizing populations, Appl. Environ. Microbiol., 63, 4704–4712, 1997.

566 Santoro, A. E., C. A. Francis, N. R. de Sieyes, and Boehm, A. B. : Shifts in the relative abundance of ammonia-oxidizing
567 bacteria and archaea across physicochemical gradients in a subterranean estuary, Environ. Microbiol., 10, 1068–1079,
568 https://doi.org/10.1111/j.1462-2920.2007.01547.x, 2008.

569 Santoro, A. E. Dupont, C. L. Richter, R. A. Craig, M. T. Carini, P. McIlvin, M. R. Yang, Y. Orsi, W. D. Moran, D. M. and
570 Saito, M. A. : Genomic and proteomic characterization of "*Candidatus Nitrosopelagicus brevis*": An ammonia-oxidizing
571 archaeon from the open ocean. Proc. Natl. Acad. Sci. USA, 112, 1173–1178, https://doi.org/10.1073/pnas.1416223112, 2015.

572 Santoro, A. E., M. A. Saito, T. J. Goepfert, C. H. Lamborg, C. L. Dupont, and DiTullio, G. R., Thaumarchaeal ecotype
573 distributions across the equatorial Pacific Ocean and their potential roles in nitrification and sinking flux attenuation. Limnol.
574 Oceanogr., 62, 1984–2003, https://doi.org/10.1002/lno.10547, 2017.

575 Schloss, P. D. Westcott, S. L. Ryabin, T. Hall, J. R. Hartmann, M. Hollister, E. B. Lesniewski, R. A. Oakley, B. B. Parks, D.
576 H. Robinson, C. J. Sahl, J. W. Stres, B. Thallinger, G. G. Van Horn, D. J. and Weber, C. F. Introducing mothur: Open-

577 Source, Platform-Independent, Community-Supported Software for describing and comparing microbial communities, Appl.
578 Environ. Microbiol., 75, 7537–7541, https://doi.org/10.1128/Aem.01541-09, 2009.

579 Sigman, D. M., K. L. Casciotti, M. Andreani, C. Barford, M. Galanter, and Bohlke, J. K. : A bacterial method for the
580 nitrogen isotopic analysis of nitrate in seawater and freshwater, Anal. Chem., 73, 4145–4153,
581 https://doi.org/10.1021/ac010088e, 2001.

582 Smith, J. M., J. Damashek, F. P. Chavez, and Francis, C. A. : Factors influencing nitrification rates and the abundance and
583 transcriptional activity of ammonia-oxidizing microorganisms in the dark northeast Pacific Ocean, Limnol. Oceanogr., 61,
584 596–609, https://doi.org/10.1002/lno.10235, 2016.

585 Vaulot, D., C. Courties, and Partensky, F. : A simple method to preserve oceanic phytoplankton for Flow Cytometric
586 Analyses, Cytometry, 10: 629–635, https://doi.org/10.1002/cyto.990100519, 1989.

587 Wankel, S. D., A. C. Mosier, C. M. Hansel, A. Paytan, and Francis, C. A. : Spatial variability in nitrification rates and
588 ammonia-oxidizing microbial communities in the agriculturally impacted Elkhorn Slough Estuary, California, Appl. Environ.
589 Microbiol., 77, 269–280, https://doi.org/10.1128/Aem.01318-10, 2011.

590 Ward, B. B. : Nitrification and ammonification in aquatic systems, Life Support Biosph. Sci., 3, 25–29, 1996.

591 Welschmeyer, N. A. : Fluorometric analysis of Chlorophyll-a in the presence of Chlorophyll-B and pheopigments, Limnol.
592 Oceanogr., 39, 1985–1992, https://doi.org/10.4319/lo.1994.39.8.1985, 1994.

593 Wu, R. N., H. Meng, Y. F. Wang, W. S. Lan, and Gu, J. D. : A more comprehensive community of ammonia-oxidizing
594 archaea (AOA) revealed by genomic DNA and RNA analyses of *amoA* gene in subtropical acidic Forest Soils, Microbiol.
595 Ecol., 74, 910–922, https://doi.org/10.1007/s00248-017-1045-4, 2017.

596 Xu, J., H. M. Jing, L. L. Kong, M. M. Sun, P. J. Harrison, and Liu, H. B. : Effect of seawater-sewage cross-transplants on
597 bacterial metabolism and diversity. Microbiol. Ecol. 66: 60–72. https://doi.org/10.1007/s00248-013-0207-2, 2013.

598 Yool, A., A. P. Martin, C. Fernandez, and Clark, D. R. : The significance of nitrification for oceanic new production. Nature,
599 447, 999–1002, https://doi.org/ 10.1038/nature05885, 2007.

600 Zhao, H.T. : Evolution of the Pearl River Estuary, China Ocean Press, Beijing, 1–357, (in Chinese), 1990

https://doi.org/10.5194/bg-2020-223
Preprint. Discussion started: 3 July 2020

10 Figures

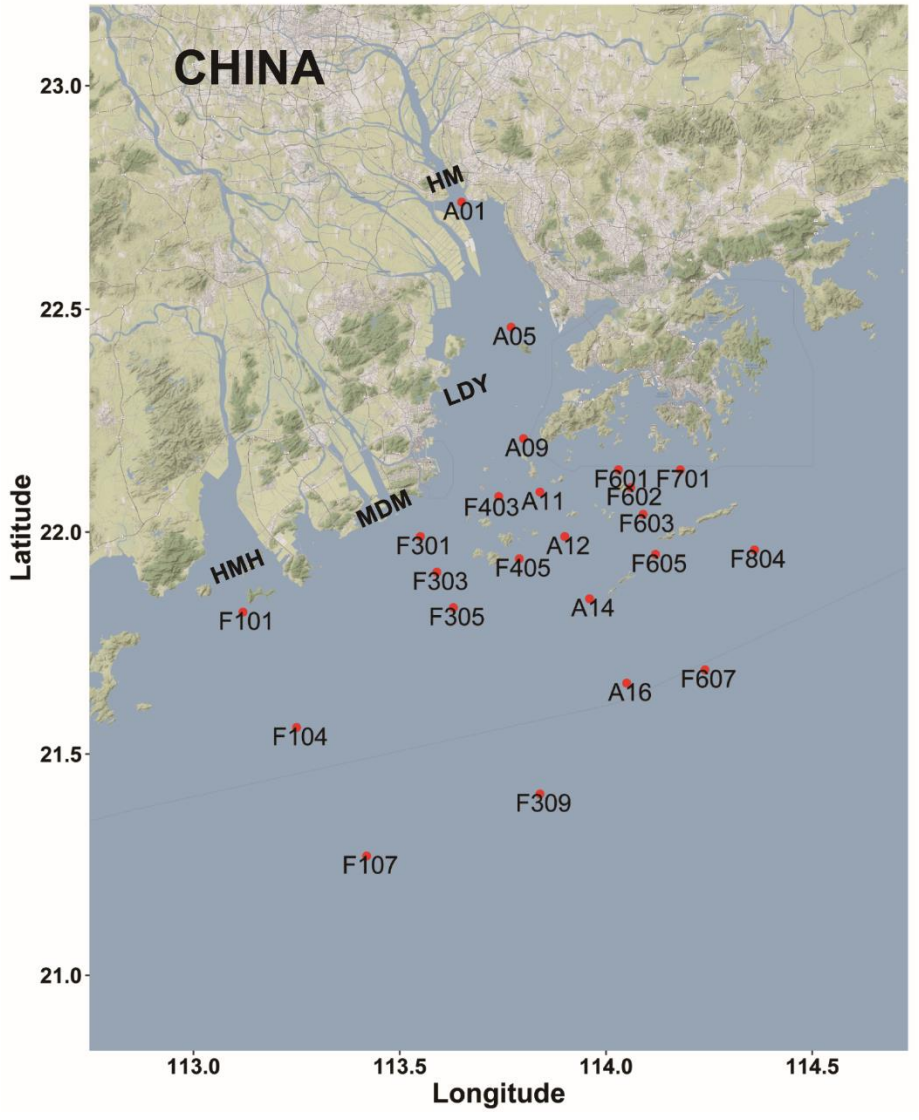

Figure 1. Sampling and rates measurement location during the Pearl River estuary cruise in 2017 summer (HMH-Huangmaohai; MDM-Modaomen; HM-Humen; LDY-Lingdingyang). The sampling location information was overlaid on Google Maps (© Google Maps) image using "ggmap" with "ggplot2" in R (D. Kahle and H. Wickham, 2013)

https://doi.org/10.5194/bg-2020-223
Preprint. Discussion started: 3 July 2020

607

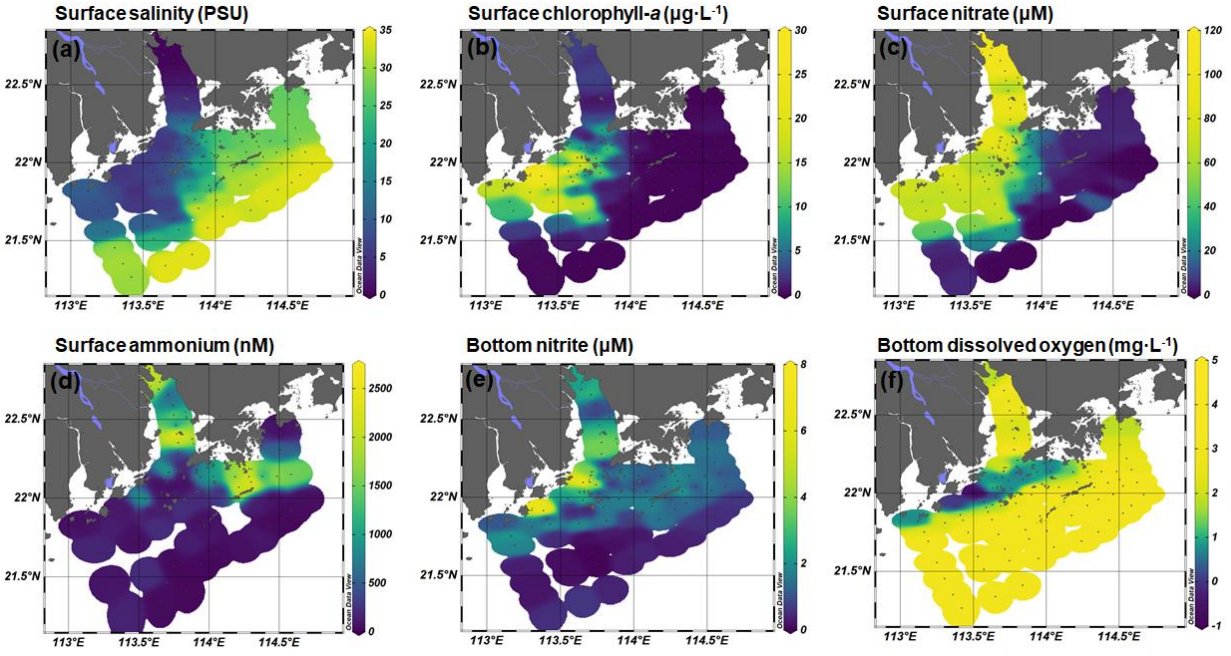

608

609 **Figure 2. Spatial distribution of (a) salinity, (b) chlorophyll-*a*, (c) nitrate, (d) ammonium at the surface layer, (e)**
610 **nitrite, and (f) dissolved oxygen concentration at bottom layer during the 2017 summer cruise in Pearl River estuary.**
611 **These figures were generated using Ocean Data View v. 5.0.0 (http://odv.awi.de).**

https://doi.org/10.5194/bg-2020-223
Preprint. Discussion started: 3 July 2020

612

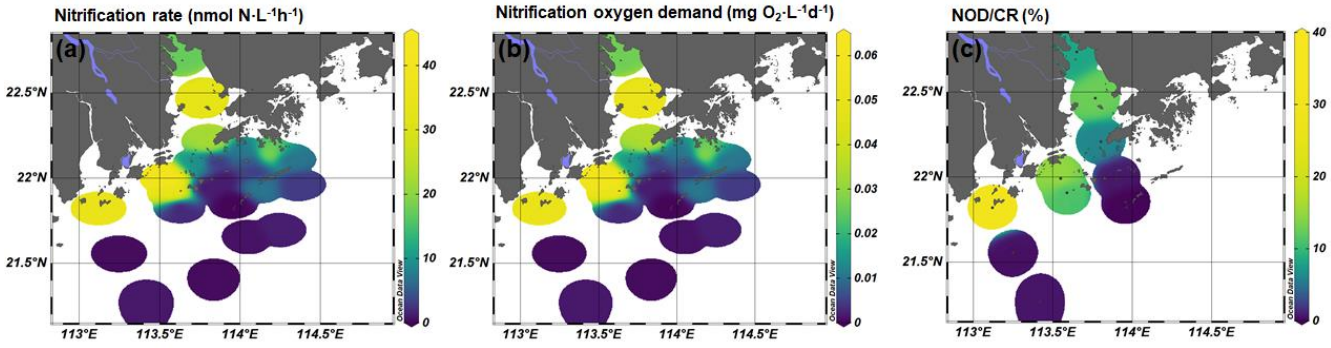

613

614 **Figure 3. (a) Nitrification rates (nmol N·L^{-1} h^{-1}), (b) nitrification oxygen demand (NOD) (mg O2·L^{-1}·d^{-1}), (c) NOD/CR**
615 **ratio (%) at the bottom layer (Data from F305 and F701 are not displayed).**

https://doi.org/10.5194/bg-2020-223
Preprint. Discussion started: 3 July 2020

616

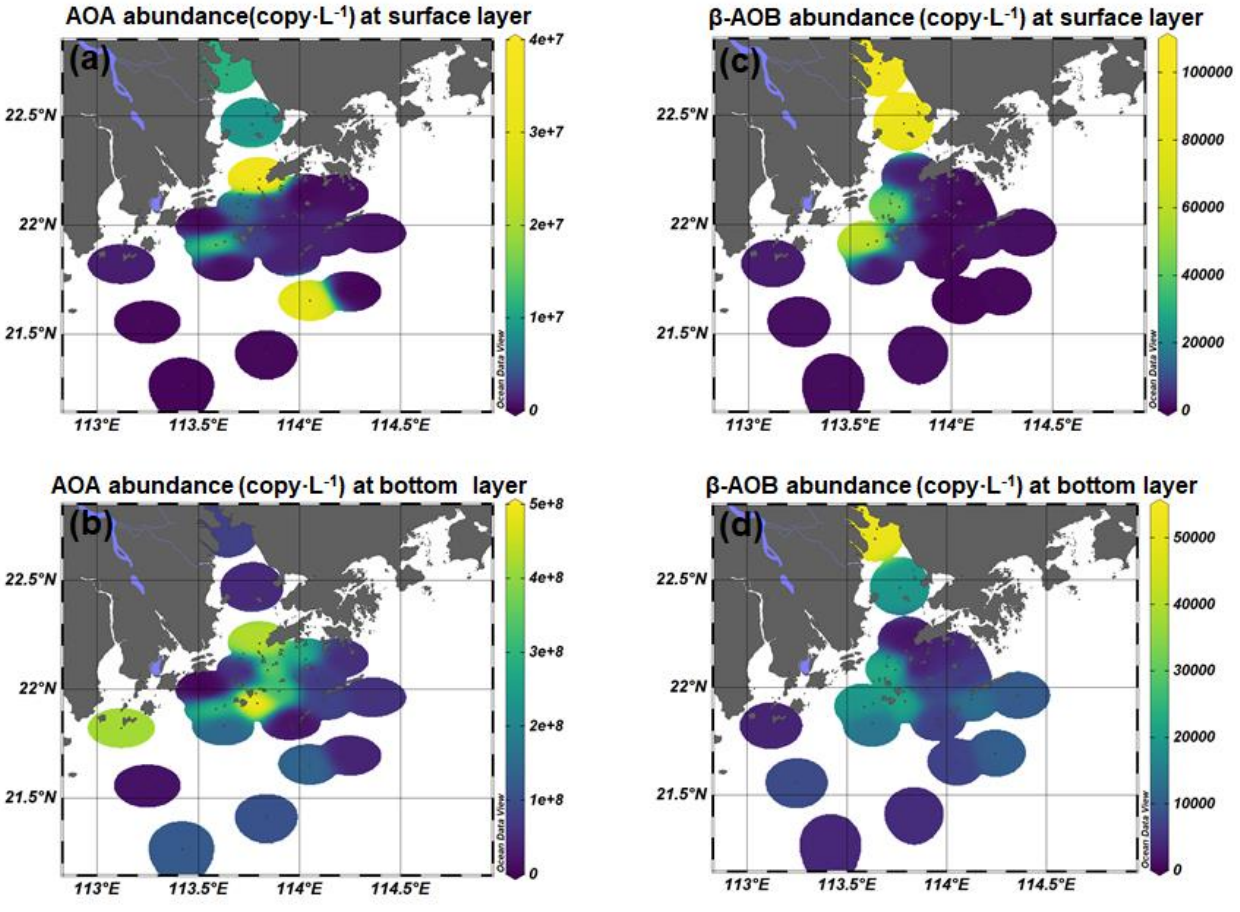

617

618 **Figure 4. Spatial distribution of AOA and β-AOB abundance at the surface and the bottom layer at DNA level.**

https://doi.org/10.5194/bg-2020-223
Preprint. Discussion started: 3 July 2020

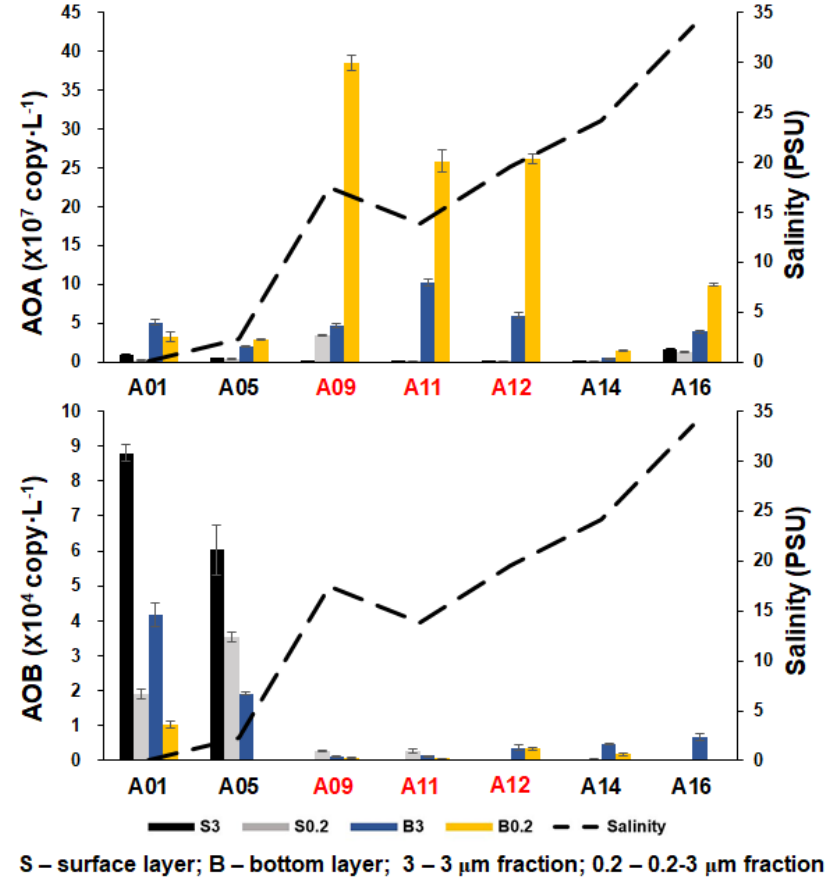

S – surface layer; B – bottom layer; 3 – 3 μm fraction; 0.2 – 0.2-3 μm fraction

Figure 5. The abundance of AOA and β-AOB at DNA level quantified by qPCR of *amoA* along the salinity gradient of the A-transect in the Pearl River estuary. Size fractionation is performed with 3 μm (particle-attached) and 0.2 μm (free-living), and the hypoxic stations (bottom DO < 2 mg·L^{-1}) are labelled in red color.

https://doi.org/10.5194/bg-2020-223
Preprint. Discussion started: 3 July 2020

Biogeosciences
Discussions
Open Access
EGU

623

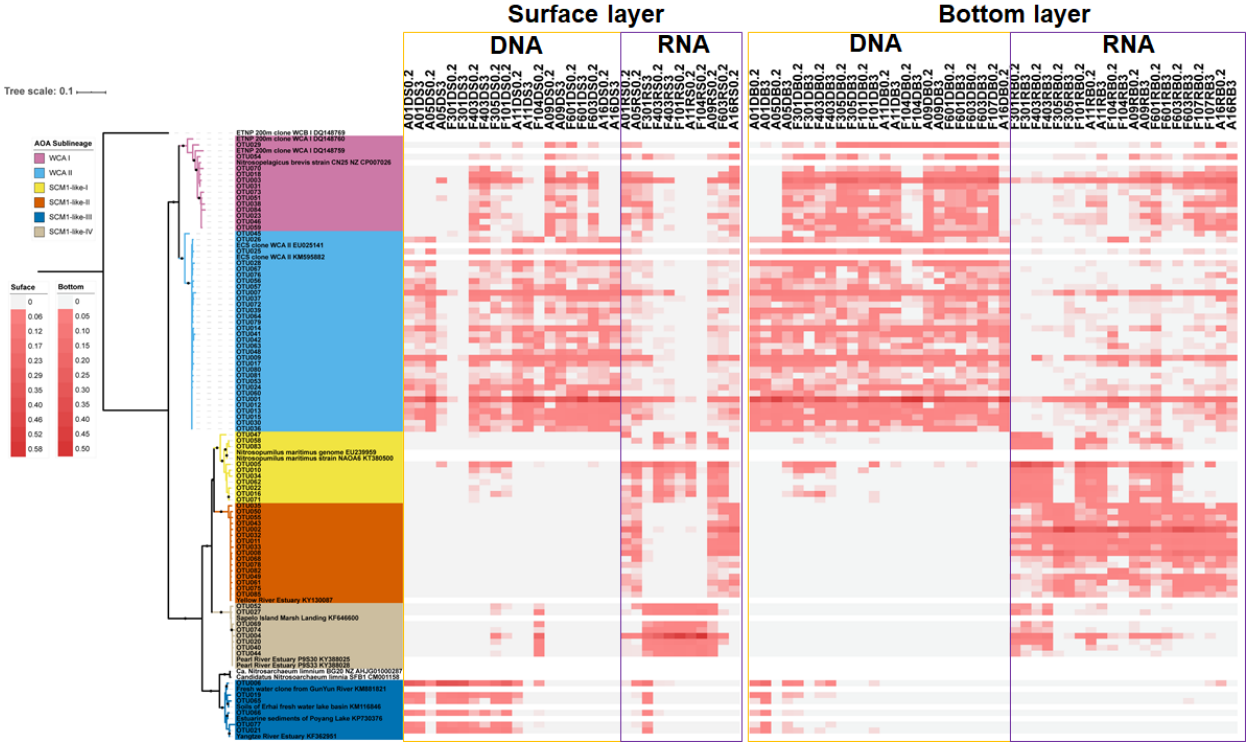

624

625 **Figure 6. Maximum likelihood phylogenetic tree of top 85 OTUs based on *amoA* gene sequences using T92+G+I**
626 **model with 1000 bootstrap. The associated heat map is generated based on the relative abundance of top OTUs.**
627 **Samples are listed from left to right along the ascending salinity gradient.**

https://doi.org/10.5194/bg-2020-223
Preprint. Discussion started: 3 July 2020

Biogeosciences
Discussions
Open Access
EGU

628

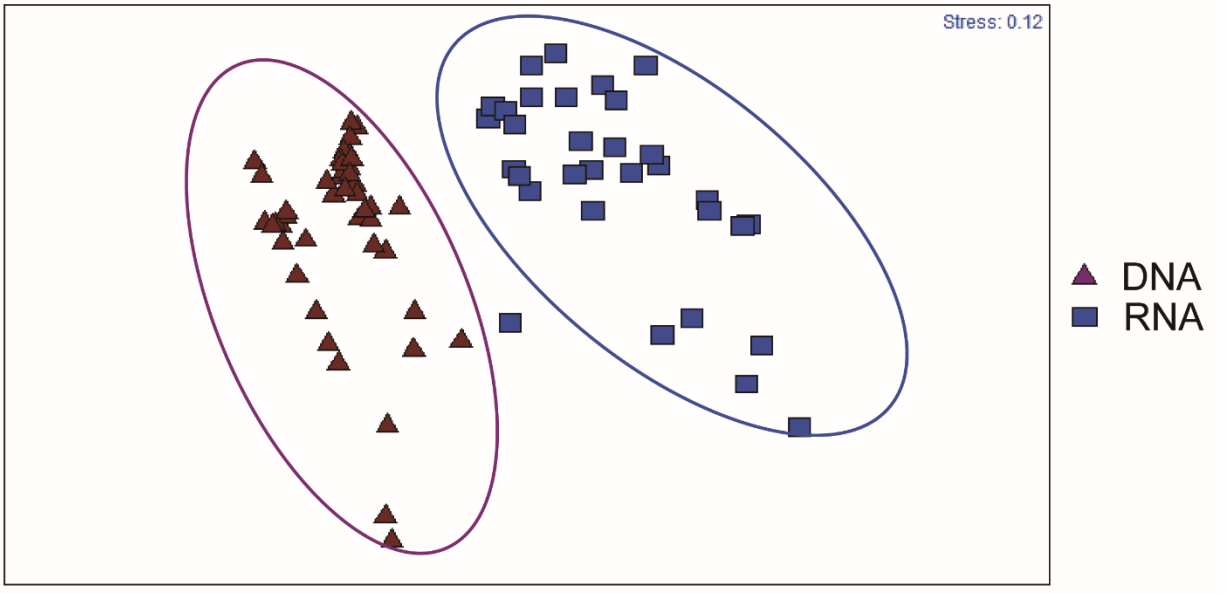

629

630 **Figure 7. Nonmetric multidimensional scaling (NMDS) plot of AOA community similarity at DNA and RNA level.**

https://doi.org/10.5194/bg-2020-223
Preprint. Discussion started: 3 July 2020

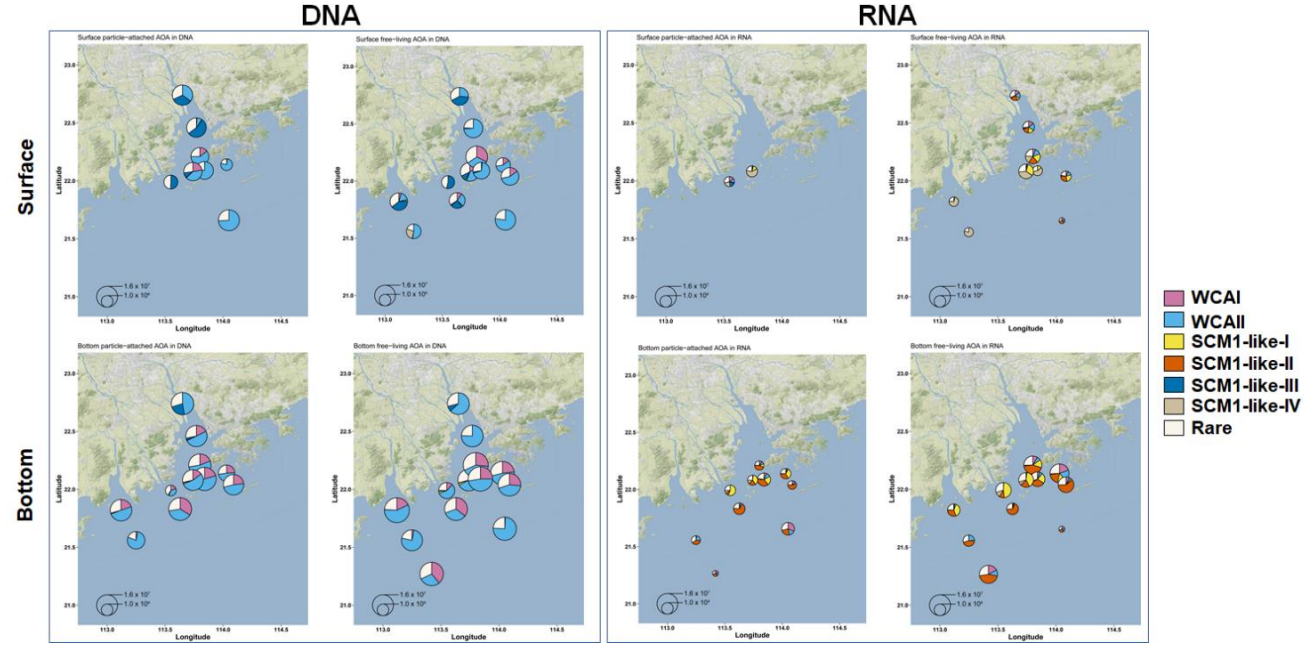

Figure 8. Free-living and particle-attached AOA community composition and distribution in the Pearl River estuary. The size of the pie charts represents the archaeal *amoA* gene abundance quantified by qPCR. For a clear display of the AOA community composition, the minimum size of the pie charts is set as 100 copies·L^{-1}. The charts were overlaid on Google Maps (© Google Maps) images using "ggmap" with "ggplot2" in R (D. Kahle and H. Wickham, 2013)

https://doi.org/10.5194/bg-2020-223
Preprint. Discussion started: 3 July 2020

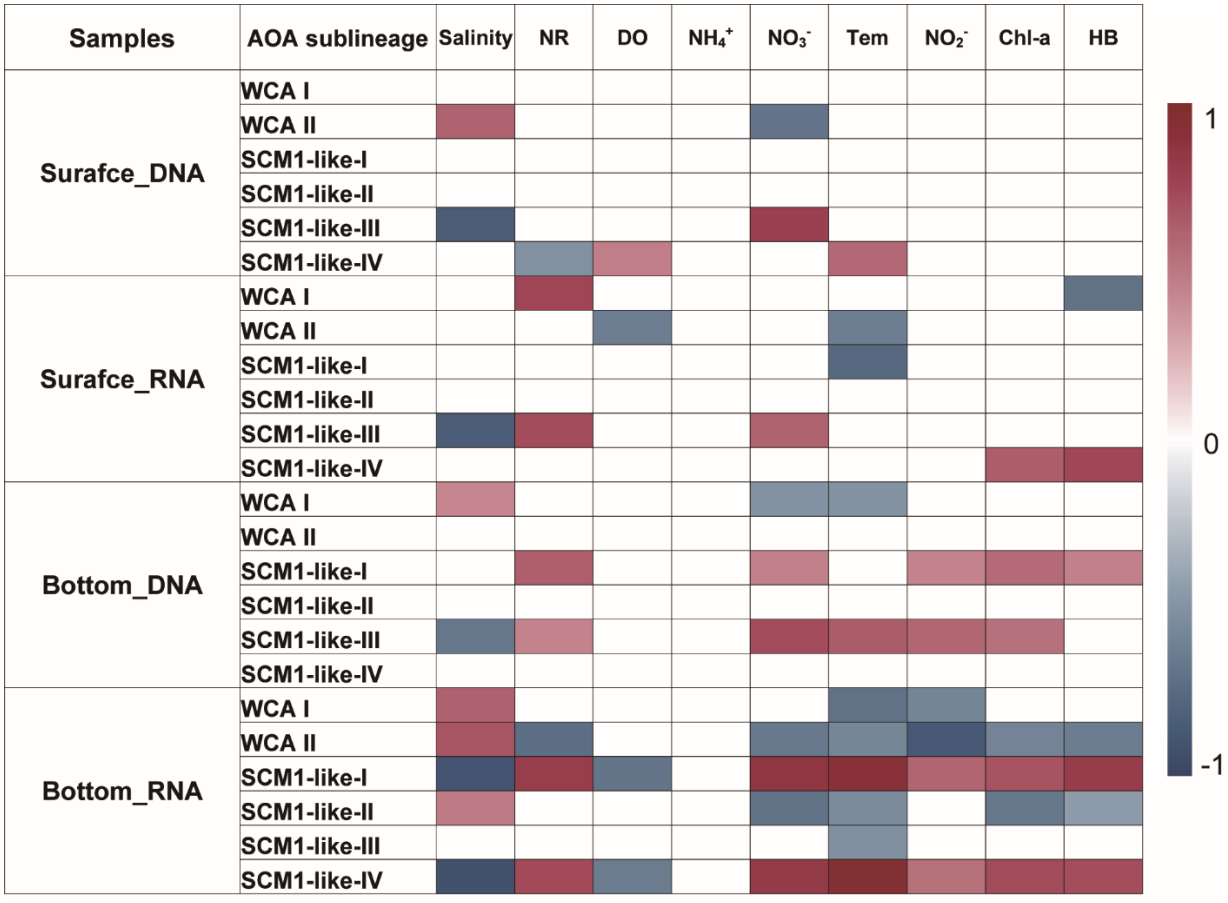

Figure 9. Spearman correlation between AOA sublineages (relative abundance at DNA and RNA levels) and environmental factors in the surface and bottom layers of the water column in the Pearl River estuary during summer 2017. Only the significant correlations (P<0.05) are displayed (NR-nitrification rates; DO-dissolved oxygen; Tem-Temperature; HB-heterotrophic bacteria abundance).